ACS APPLIED MATERIALS & INTERFACES

Research Article

www.acsami.org

Pressure-Assisted Synthesis of HKUST-1 Thin Film on Polymer Hollow Fiber at Room Temperature toward Gas Separation

Yiyin Mao,[†] Junwei Li,[†] Wei Cao,[†] Yulong Ying,[†] Luwei Sun,[†] and Xinsheng Peng*[,†,‡]

[†]State Key Laboratory of Silicon Materials, Department of Materials Science and Engineering, Zhejiang University, Hangzhou, Zhejiang 310027, P. R. China

[‡]Cyrus Tang Center for Sensor Materials and Application, Department of Materials Science and Engineering, Zhejiang University, Hangzhou, Zhejiang 310027, P. R. China

Supporting Information

ABSTRACT: The scalable fabrication of continuous and defect-free metal-organic framework (MOF) films on the surface of polymeric hollow fibers, departing from ceramic supported or dense composite membranes, is a huge challenge. The critical way is to reduce the growth temperature of MOFs in aqueous or ethanol solvents. In the present work, a pressure-assisted room temperature growth strategy was carried out to fabricate continuous and well-intergrown HKUST-1 films on a polymer hollow fiber by using solid copper hydroxide nanostrands as the copper source within 40 min. These HKUST-1 films/polyvinylidenefluoride (PVDF) hollow fiber composite membranes exhibit good separation performance for binary gases with selectivity 116% higher than Knudsen values via both inside-out and outside-in modes. This provides a new way to enable for scale-up preparation of HKUST-1/polymer hollow fiber membranes, due to its superior economic and ecological advantages.

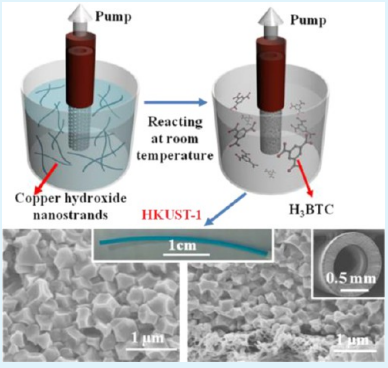

KEYWORDS: *metal-organic framework membrane, polymer hollow fiber, seed-free, room temperature, pressure-assisted*

INTRODUCTION

Metal-organic framework (MOF) materials,[1−3] due to their unique porous structures and diverse properties, have attracted significant attention for constructing high separation performance membranes.[4−9] Various methods have been carried out to grow continuous MOF membranes.[9−18] Most of them were in flat sheet modules on porous substrates and grown through the secondary seeding process under the hydro/solvent thermal condition at relatively high temperature, typically above 100 °C.[19,20] However, due to its space-saving setup property, the hollow fiber module is widely used in the industrial scale.[19,20] In order to reach this industrial demand, MOF membranes in hollow fiber module, namely, a MOF skin (or barrier) layer on hollow fiber support, are strongly requested. Recently, several MOF membranes supported on ceramic hollow fibers have been grown by the seeding process,[10−12,14−18] due to the high thermal stabilities of ceramic supports, which could sustain the hydro/solvent thermal conditions for MOF growth. However, MOFs/ceramic hollow fiber membranes currently have limited applications, due to the high cost of the ceramic support and difficulties in the scale-up and reliability of hydrothermal growth.

It is well-known that polymer hollow fibers are much cheaper than ceramic hollow fibers and widely used in industrial separation processing. However, the main drawbacks of them are their low thermal stability and weak organic resistance at high temperature, since most of the MOFs were grown in organic solvents at high temperature, containing metal salts with organic or inorganic acidic groups for a long time.[19,20] These will make the process cost consuming and environmentally unfriendly. In addition, cracks will easily form during the cooling process due to the different thermal expansion between MOFs and the supports. Therefore, the scalable fabrication of continuous and defect-free MOF membranes on the surface of polymeric hollow fibers, departing from ceramic supported or dense composite membranes, is a huge challenge. The most important way is to reduce the growth temperature of MOFs in aqueous or ethanol solvents. Up to date, only Brown et al. recently obtained continuous ZIF-90 membranes on polymeric hollow fiber at 65 °C through a dip-coating seeding layer by a secondary growth in methanol.[11]

Very recently, we found that at room temperature free-standing HKUST-1 intergrown continuous flat membranes could be prepared by reacting copper hydroxide nanostrand (CHN) thin films with 1,3,5-benzenetricarboxylic acid (trimesic acid, H_3BTC) water/ethanol solution.[21] Although the flat sheet structure of the prepared HKUST-1 membranes has a limitation for the most used spiral wound modules and hollow fiber modules, the synthesis provides a great chance to grow HKUST-1 film on polymer hollow fiber at room temperature. Herein, we presented a way to rapidly synthesize continuous HKUST-1 membranes on polyvinylidenefluoride (PVDF)

Received: January 12, 2014
Accepted: March 5, 2014
Published: March 5, 2014

hollow fibers through a pressure-assisted seed-free growth process by using copper hydroxide nanostrand thin films as the copper source at room temperature. PVDF is chemically resistant, withstands high temperature (up to 177 °C), and has a low density (1.78) and low cost compared to the other fluoropolymers.[22] A 6.5 μm thick HKUST-1 film composed of a 3 μm thick continuous, well-intergrown, and dense surface layer on a PVDF hollow fiber was obtained within only 40 min. The prepared HKUST-1 coated PVDF hollow fiber membranes demonstrated nice separation performance for binary gases via both inside-out mode and outside-in modes. This provides a new scale-up fabrication for HKUST-1/polymer hollow fiber membranes, except for the previously reported formation of MOFs/ceramic hollow fibers by using organic solvents and metal salts at high temperature and a long time.[10−12,14−18]

EXPERIMENTAL SECTION

Preparation of CHNs. CHNs were synthesized by quickly mixing an equal volume of 2 mM copper nitrate (Acros Chemicals) and 0.7 mM aminoethanol (Acros Chemicals) at room temperature and aged for 2 days.[23]

Preparation of Continuous HKUST-1 Membranes on PVDF Hollow Fibers. First, a mesoporous CHN layer was prepared by filtering certain CHNs on PVDF hollow fibers (Tianjin Motimo Membrane Technology CO., LTD). The porosity of these hollow fibers is 40−60% with pore size of about 200 nm. One end of the PVDF hollow fiber was inserted by a pinhead which directly connected the pump while the other side was sealed by Teflon tape. After filtering for 30 min, the PVDF hollow fiber with CHN layer was put into a container, which contained 20 mL of a 20 mM H_3BTC (Sigma-Aldrich) ethanol/water solution with volume ratio of 1:1 and kept reacting at room temperature without turning off the pump. The color turned from light blue of the CHN layer to dark blue after a few minutes. Typically, after 40 min, a continuous HKUST-1 membrane on PVDF hollow fiber was obtained and used for gas separation. The parameters, including reaction time and concentration of H_3BTC, were investigated in detail (see Supporting Information).

Characterization. X-ray diffraction pattern (XRD) was carried out by an X'Pert PRO (PANalytical, Netherlands) instrument with Cu Kα radiation at room temperature. The morphologies and structures were characterized by using scanning electron microscopy (SEM; Hitachi S-4800), and SEM observation was conducted after coating a thin platinum layer by using a Hitachi e-1030 ion sputter at the pressure of 10 Pa and the current density of 10 mA. The gas permeation was carried out by using a homemade hollow fiber separation system with mass flow meters (Seven-star D07-19BM) and gas chromatography (see Scheme S1, Supporting Information). Before gas permeation measurements, the modules were heated from room temperature to 100 °C at a rate of 20 °C·h^{-1} and held for 0.5 h and then cooled to room temperature at the same rate. After that, the activated HKUST-1 membrane was tested by gas permeation experiments in both gas outside-in and inside-out modes (see Scheme S1, Supporting Information).

RESULTS AND DISCUSSION

Scheme 1 shows the pressure-assisted preparation process of HKUST-1 membranes on the outside surface of PVDF hollow fiber. First of all, a CHN layer was precoated on the outside surface of the PVDF hollow fiber by sealing one end with suction filtration. Then, continuous HKUST-1 membranes were grown by immersing the precoated PVDF hollow fiber with the CHN layer into a H_3BTC ethanol/water solution with a volume ratio of 1:1 at room temperature for a certain time. During the transferring and growing processes, an external pressure of 90 kPa was applied by the vacuum pump. The PVDF hollow fiber has an outer diameter of 1 mm and inner

Scheme 1. Preparation Process of HKUST-1 Membrane on the Surface of PVDF Hollow Fibers[a]

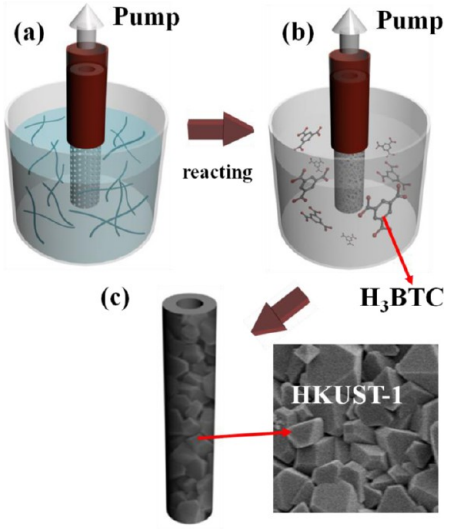

[a](a) Filtering CHNs on PVDF hollow fibers. (b) After filtering for 30 min, reaction with 20 mL of a 20 mM H_3BTC ethanol/water solution with a volume ratio of 1:1 at room temperature, and (c) after a certain time, HKUST-1 layers were formed on the PVDF hollow fiber support. A vacuum pressure of 90 kPa was kept during the whole process.

diameter of 0.6 mm with a typical porous skin layer (Figure 1a,b). The CHN nanofibrous layer on the outside surface of the PVDF hollow fiber was mesoporous with thickness of about 2 μm as shown in Figure 1c,d. In our case, the effective length of the PVDF hollow fiber was 5 cm. After putting the CHN-precoated PVDF hollow fiber into 30 mL of a 20 mM H_3BTC water/ethanol solution with volume ratio of 1:1 at room temperature for 5 min, the SEM images in Figure 2a shows that the HKUST-1 crystals are randomly formed without obvious intergrowth. The high magnification magnification image (inset in Figure 2a) clearly shows the nanofibrous structures, which are the unreacted CHNs. This means that the reaction starts from the most-outer surface part of the CHN layer. The corresponding XRD patterns of the HKUST-1 films (Figure 3b) indicate that pure HKUST-1 is formed even just for 5 min. When the reaction time increased to 20 min, dense HKUST-1 film is continuously formed on the PVDF hollow fiber, as shown in Figure 2b. Finally, after reacting for 40 min, Figure 2c−d shows that a continuous HKUST-1 film with a thickness of about 6.5 μM is formed on the outside surface of PVDF hollow fiber. No visible pinhole or crack is observed. Noting that this HKUST-1 film is composed of a less intergrown bottom layer and a dense and well-intergrown upper layer, the dense and well-intergrown upper layer is about 3 μM, which is responsible for the gas separation performance. The possible reason for this hierarchical structure is that BTC ligands would first react with the CHNs on the top surface CHN layer. While the time went on, the well-intergrown membrane formed on the top layer while the BTC ligands hardly went into the bottom CHN layer. The HKUST-1 clusters forming at the bottom may not be sufficient to grow into big crystals. Some of them diffuse to the preformed HKUST-1 crystals at the top surface and help in the formation of well-intergrown HKUST-1

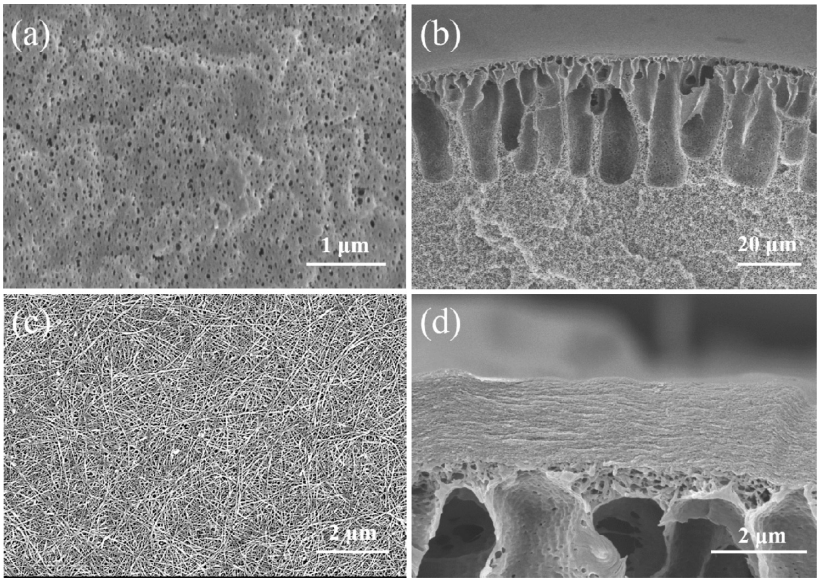

Figure 1. SEM images of the (a) surface and (b) cross section of the PVDF hollow fibers; (c) surface and (d) cross section of the CHN layer coated PVDF hollow fiber.

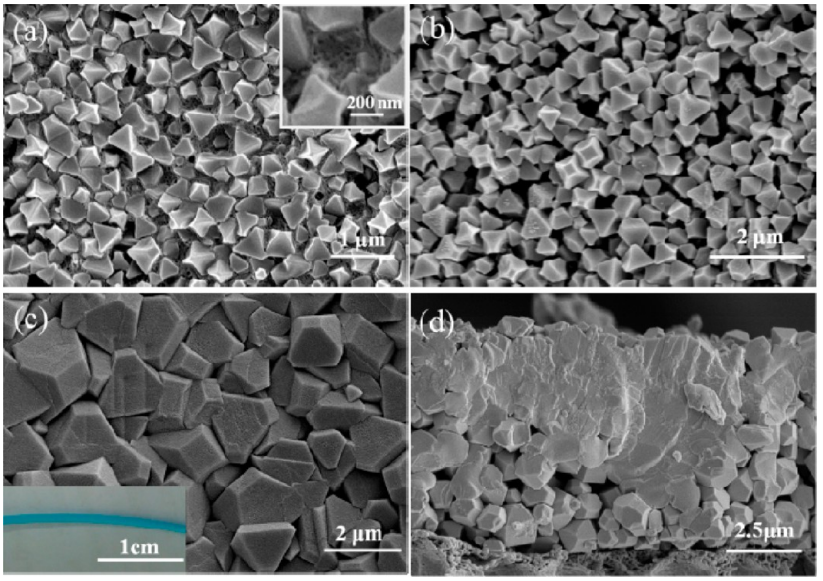

Figure 2. SEM images of the HKUST-1 layer coated PVDF hollow fibers, prepared from 30 mL of 20 mM H_3BTC at room temperature for (a) 5 min, (b) 20 min, and (c) and (d) 40 min, respectively. The inset is magnified from (a) and the corresponding photo image of the sample is shown in c.

crystals. The others may generate new nucleates and grow into new crystals, due to fewer nutrients reaching the bottom CHN layer, which turned out to be the loosely packed porous structure at the bottom. This is confirmed by SEM in Figure 2a−c. Low-magnification view SEM images (Figure S1a−c, Supporting Information) indicate that the HKUST-1 film completely and uniformly covers the outside surface of the PVDF hollow fiber. The XRD pattern (Figure 3b,c,e) prepared for different times indicates that pure HKUST-1 is formed without any secondary phase.

Figure 4a−c presents HKUST-1 films synthesized on the surface of PVDF hollow fiber after reacting with 30 mL of a 10 mM H_3BTC ethanol/water solution with volume ratio of 1:1 at room temperature for 40 min. It is obvious that the crystals are not completely intergrown and grain boundaries can be clearly seen. Although we used the same amount of CHNs, the thickness of this membrane, which is over 10 μm, is greater than that in the 20 mM H_3BTC case. That is to say, the membrane in this case is much looser and there is much more interspace than in the 20 mM one. The corresponding XRD patterns of the HKUST-1 films (Figure 3b) indicate that pure HKUST-1 is formed without any secondary phase.

Since all the reactions were processed under an external pressure of 90 kPa as shown in Scheme 1, the transferring volume of H_3BTC solution through the system should reflect the reaction speed and the quality of the HKUST-1 films. Figure 5 shows the corresponding transferring volume of H_3BTC solutions with different concentrations and reacting with the same thick CHN layers under pressure of 90 kPa. It is clear that, in the case of 20 mM H_3BTC solution, the solution

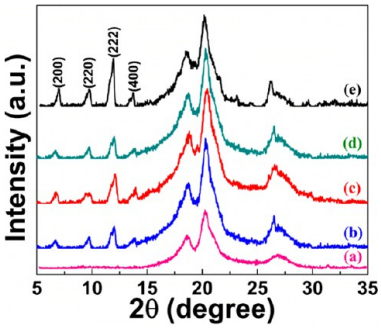

Figure 3. XRD patterns of (a) bare PVDF hollow fibers and the HKUST-1 films formed on the PVDF fibers for (b) 5 min, (c) 20 min, and 40 min (e) from 30 mL of 20 mM H_3BTC at room temperature, respectively, and (d) from 30 mL of 10 mM H_3BTC at room temperature for 40 min.

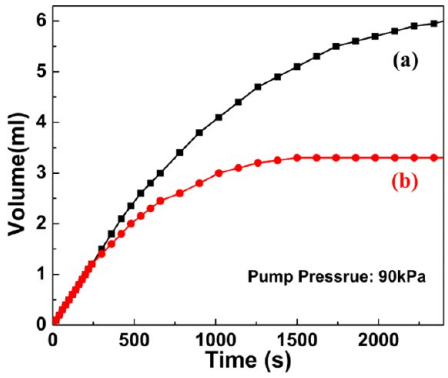

Figure 5. The permeating volume of the solution through the hollow fibers during HKUST-1 vs time. (a) 10 mM and (b) 20 mM reacting with CHNs at room temperature under a pressure of 90 kPa, respectively. All the data are averaged from the five measured points under the same test conditions. The average errors in all the data are about 4%.

transferring speeds is almost the same at the beginning 5 min. With the time elongation, the transferring rates slow down and are at last almost close to zero. However, in the case of 10 mM H_3BTC solution, the decrease of the transferring rates is dramatically slower than that of the 20 mM solution. In addition, the transferring amount of 10 mM H_3BTC solution is about 5 mL after 25 min, which is much higher than 3 mL of the 20 mM H_3BTC solution. The starting block time for 20 mM H_3BTC solution is about 1100 s while in the 10 mM case there is hardly a starting block time. The HKUST-1 film prepared at 20 mM H_3BTC solutions after 40 min are solvent impermeable. This further indicates that the macro-defects-free HKUST-1 films are formed. However, in the 10 mM case, the liquid permeance could not be completely blocked even for a very long time, due to the nonwell-intergrown HKUST-1 film. Therefore, it is easy to draw the conclusion that the reaction rate in 20 mM H_3BTC is faster than that in 10 mM H_3BTC, which results in a HKUST-1 film with a well-intergrown most-outer surface layer on the PVDF hollow fiber support.

We further found that the external pressure is the key point to achieve highly intergrown, continuous, and robust HKUST-1 films on the curvature surface of polymer. Without pressure, no continuous HKUST-1 films could be obtained. The pressure could make the CHN layer have a uniform thickness[24] and firmly adhere on the PVDF surface and hold the following formed HKUST-1 crystals by reacting CHNs with H_3BTC tightly grown on the hollow fiber surface. In addition, the pressure process also will self-adjust the local permeance, namely, the amount of the H_3BTC into the CHN layer at the beginning and accelerate the H_3BTC diffusion, then shorting the formation time to 40 min. It is much shorter than 2 h for the formation of the HKUST-1 flat sheet membrane with similar thickness by using the same thick CHN layer without pressure.[21]

After activating (see Experimental Section), the highly continuous HKUST-1 coated PVDF hollow fiber with a 6.5 μm thick HKUST-1 film (shown in Figure 2c) was used to investigate the gas separation. This film is homogeneous and continuous without any visible gap, pinhole, or crack. Figure S2, Supporting Information, shows the single gas permeance through the bare PVDF hollow fiber. It is clear that bare PVDF hollow fiber does not have obvious gas selectivity due to its large pores. The permeance of gas through the HKUST-1 film coated PVDF hollow fiber (shown in Figure 6a) is 2 orders of magnitude lower than that of bare PVDF hollow fiber but with Knudsen selectivity for a single gas. The permeance of H_2 is 2.01×10^{-6} mol·m^{-2}s^{-1}Pa^{-1}, which is much higher than that of CH_4, N_2, O_2, and CO_2. This further indicates that the HKUST-1 film is well-intergrown and firmly adheres on the PVDF surface as it is not broken when the gas flows via inside-out mode (Scheme 2a) under applied pressure up to 2 bar. The permeances of these gases are independent of the pressure drops, indicating the absence of macroscopic defects.[25] Similarly, Figure 6c shows the single gas permeance through the same membrane while the gas flows via outside-in mode (Scheme 2b). The performances are almost the same as those flowing via inside-out mode (Scheme 2a). For single components permeation, the ideal separation factors of this membrane for H_2/CH_4, H_2/N_2, H_2/O_2, and H_2/CO_2 are 2.5, 3.3, 3.4, and 4.2, respectively, which approaches the corresponding Knudsen selectivity (Figure 6b,d). This is reasonable since the pore size of HKUST-1 crystal (ca. 9 Å)

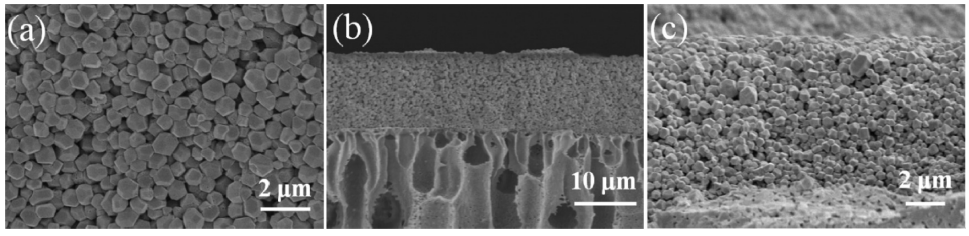

Figure 4. SEM images of the (a) surface and (b, c) cross section of the HKUST-1 film formed on the PVDF hollow fiber, from 30 mL of 10 mM H_3BTC at room temperature for 40 min.

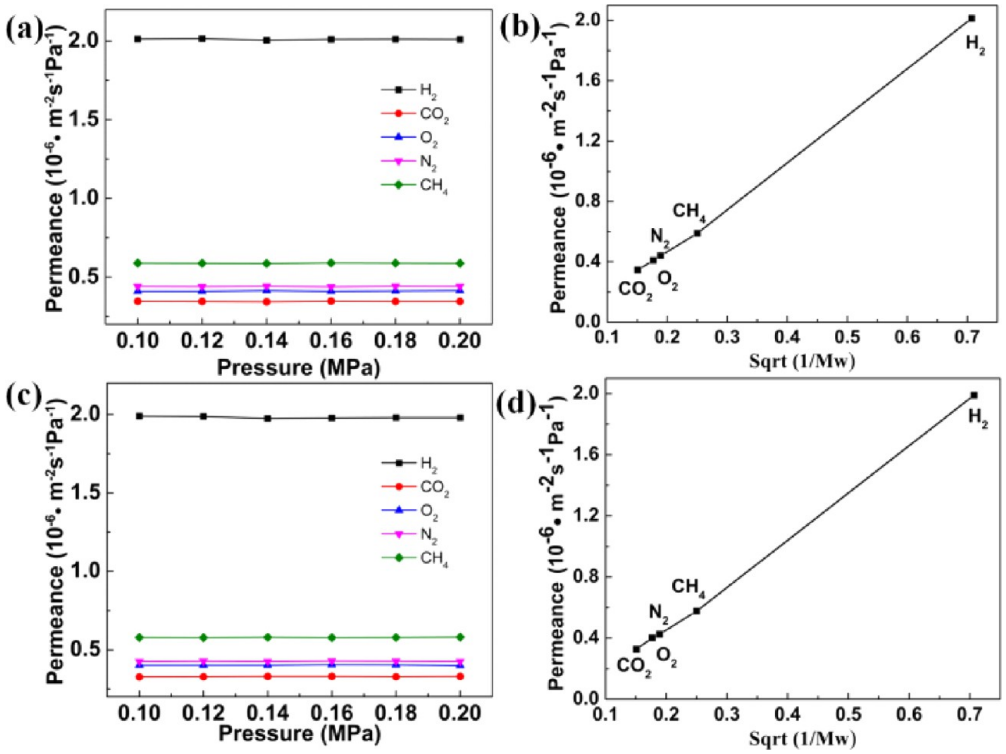

Figure 6. Single gas permeance through the prepared HKUST-1 layer coated PVDF hollow fiber (Figure 2c) under different pressure and single gas permeance as a function of the inversion of the square of the molecular weight. The gas flows from the inner to the outside surface (a, b) and from the outside to the inner channel (c, d) (see in Scheme 2), respectively. All the data are averaged from the five measured points under the same test conditions. The average errors in all the data are about 6%.

Scheme 2. The Gas Separation Processed in Both (a) Inner to Outside Mode and (b) Outside to Inner Channel Mode[a]

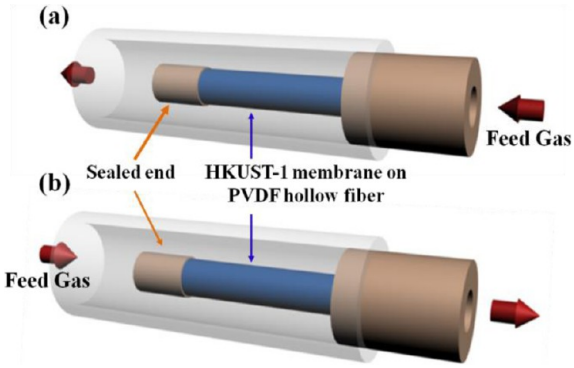

[a]The outlet was connected with a gas flow and then branched to a gas chromatography.

is much larger than the kinetic diameters of H_2 (2.9 Å), O_2 (3.46 Å), N_2 (3.6 Å), CO_2 (3.3 Å), and CH_4 (3.8 Å).[26]

However, the separation factors of the binary gases with vol/vol of 50:50 H_2/CH_4, H_2/N_2, and H_2/CO_2 are 5.4, 6.5, and 8.1, respectively, with permeance of 1.97×10^{-6} mol·m^{-2}s^{-1}Pa^{-1}. These values exceed the ideal Knudson selectivity of 2.8, 3.7, and 4.7 of the corresponding binary gases, respectively. This might be due to the influences of both the sorption and size effect as mentioned by Zhu et al.[27] The HKUST-1 coated PVDF hollow fiber membrane retains its separation factors and permeation more than 24 h, as shown in Figure 7a (gas flows via inside-out mode, Scheme S1a, Supporting Information) and Figure 7b (gas flows via outside-in mode, Scheme 2b). The membrane can be used repeatedly over three months in the present study. To make a comparison, the available experimental data related to the permeance of single gas and the binary gas separation factors in the MOF membranes are given in Table 1.[5,8,18,21,25,27−34] When compared to the HKUST-1 membrane on the surface of the Al_2O_3 tube in ref 17 and HKUST-1 on the Cu net in ref 25, the separation factors of the HKUST-1 membranes prepared here are a little lower than those in their work while our permeation fluxes are higher than theirs. The ideal separation membrane requires both high permeation flux and selectivity. Our membrane also has a comparable efficiency to other MOFs like ZIF-8 and ZIF-90, in gas separation.

CONCLUSION

In summary, this work demonstrates that continuous intergrown HKUST-1 film can be scale-up synthesized on the curved surface of the PVDF hollow fibers within 40 min at room temperature by using CHNs as the solid copper source through a pressure-assisted process. Both the gas separation factors and permeance of the as-prepared highly intergrown HKUST-1 membranes are higher than those reported in previous literature on ceramic-supported HKUST-1 membranes.[26,28,32] This separation factor of binary H_2/CO_2 is 93% to 116% higher than the Knudsen selectivity. The room temperature seed-free and salt-free process provides a new convenient and effective route for preparing MOF membranes on the surface of polymeric hollow fibers.

dx.doi.org/10.1021/am500233m | ACS Appl. Mater. Interfaces 2014, 6, 4473−4479

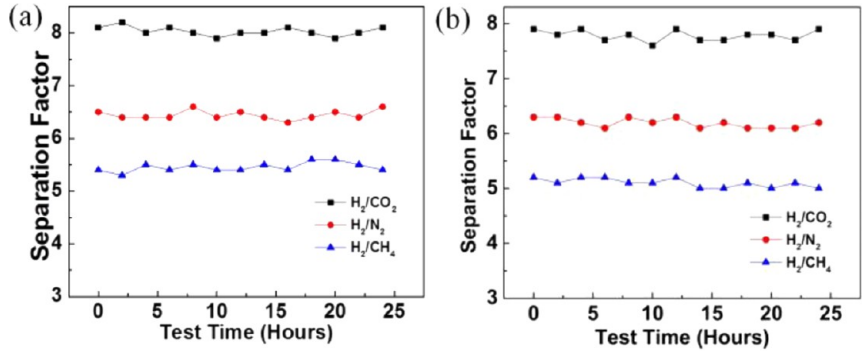

Figure 7. Plot of H_2/N_2, H_2/CH_4, and H_2/CO_2 binary gas separation factors through the prepared HKUST-1 layer coated PVDF hollow fiber (Figure 2c). The gas flows (a) from the inner channel to the outside surface and (b) from the outside to the inner channel, respectively. All the data are averaged from the five measured points under the same test conditions. The average errors in all the data are about 5%.

Table 1. Comparison of the Selectivity and Permeation Properties in the MOF Membrane

	synthesis		permeance (mol × 10^{-6} m^{-2} s^{-1} pa^{-1})				separation factor					
MOF	T (°C)	time (h)	H_2	CO_2	N_2	CH_4	H_2/CO_2	H_2/N_2	H_2/CH_4	thickness (μm)	support	ref
MOF-5	105	9	0.8	0.25	0.3	0.39	3.2	2.67	2.05	40	Al_2O_3	25
ZIF-8	100	4	0.06	0.013	0.005	0.005	6.73	12	12	40	TiO_2	5
ZIF-7	100	3	0.074	0.011	0.011	0.012	6.7	6.7	6.2	1.5	Al_2O_3	8
ZIF-8	30	6	0.36	0.14	0.09	0.08	2.57	4	4.5	2.5	Al_2O_3	33
ZIF-90	65	4	0.19	0.104	0.03	0.07	1.8	6.3	2.7	5	Torlon	11
ZIF-90	100	18	0.21	0.013	0.012	0.011	16.15	17.5	19.09	20	Al_2O_3	29
ZIF-90	100	18	0.25	0.035	0.019	0.016	7.14	13.16	15.63	20	Al_2O_3	30
ZIF-95	120	72	2	0.076	0.216	0.185	25.7	10.2	11	30	Al_2O_3	34
HKUST-1	100	48	0.036	0.003	0.003	0.032	9.1	9.9	7.6	13	Al_2O_3	18
HKUST-1	120	72	0.127	0.028	0.028	0.016	6.84	7.04	5.92	60	Cu Net	27
HKUST-1	120	6	2	0.5	0.5	0.8	3.5	3.7	2.4	25	Al_2O_3	32
HKUST-1	120	12	0.748	0.148	0.203	0.257	5.1	3.7	2.9	25	Al_2O_3	28
HKUST-1	25	2	1.59	0.385	0.47	0.637	4.7	3.7	2.8	4.5	none	21
HKUST-1	120	24	0.186	0.039	0.043	0.059	6.9	5.8	4.9	50	Al_2O_3	31
HKUST-1	25	0.667	2.01	0.35	0.44	0.59	8.1	6.5	5.4	3	PVDF	this work[a]

[a]The data are averaged from the five measured points under the same test conditions with average errors of about 5%.

■ ASSOCIATED CONTENT

Supporting Information

Figures of the SEM images of the membrane and gas separation performance of bare PVDF hollow fiber. This information is available free of charge via the Internet at http://pubs.acs.org/.

■ AUTHOR INFORMATION

Corresponding Author

*E-mail: pengxinsheng@zju.edu.cn.

Notes

The authors declare no competing financial interest.

■ ACKNOWLEDGMENTS

This work was partially supported by the National Nature Science Foundations of China (NSFC 21271154), Ninbo Oulin Kitchen Utensils Co. Ltd, Doctoral Fund of Ministry of Education of China (20110101110028), and The Project-sponsored by SRF for ROCS, SEM.

■ REFERENCES

(1) Kong, G.-Q.; Han, Z.-D.; He, Y.; Ou, S.; Zhou, W.; Yildirim, T.; Krishna, R.; Zou, C.; Chen, B.; Wu, C.-D. Expanded organic building units for the construction of highly porous metal−organic frameworks. *Chem.—Eur. J.* **2013**, *19* (44), 14886−14894.

(2) Shekhah, O.; Liu, J.; Fischer, R.; Wöll, C. MOF thin films: Existing and future applications. *Chem. Soc. Rev.* **2011**, *40* (2), 1081−1106.

(3) Zhou, H.-C.; Long, J. R.; Yaghi, O. M. Introduction to metal-organic frameworks. *Chem. Rev.* **2012**, *112* (2), 673−674.

(4) Bétard, A. l.; Fischer, R. A. Metal-organic framework thin films: From fundamentals to applications. *Chem. Rev.* **2012**, *112* (2), 1055−1081.

(5) Bux, H.; Liang, F.; Li, Y.; Cravillon, J.; Wiebcke, M.; Caro, J. Zeolitic imidazolate framework membrane with molecular sieving properties by microwave-assisted solvothermal synthesis. *J. Am. Chem. Soc.* **2009**, *131* (44), 16000−16001.

(6) Bae, T. H.; Lee, J. S.; Qiu, W.; Koros, W. J.; Jones, C. W.; Nair, S. A high-performance gas-separation membrane containing submicrometer-sized metal-organic framework crystals. *Angew. Chem., Int. Ed.* **2010**, *49* (51), 9863−9866.

(7) Li, Y. S.; Bux, H.; Feldhoff, A.; Li, G. L.; Yang, W. S.; Caro, J. Controllable synthesis of metal-organic frameworks: From MOF nanorods to oriented MOF membranes. *Adv. Mater.* **2010**, *22* (30), 3322−3326.

(8) Li, Y. S.; Liang, F. Y.; Bux, H.; Feldhoff, A.; Yang, W. S.; Caro, J. Molecular sieve membrane: Supported metal-organic framework with high hydrogen selectivity. *Angew. Chem., Int. Ed.* **2010**, *49* (3), 548−551.

(9) Meek, S. T.; Greathouse, J. A.; Allendorf, M. D. Metal-organic frameworks: A rapidly growing class of versatile nanoporous materials. *Adv. Mater.* **2011**, *23* (2), 249−267.

(10) Aguado, S.; Nicolas, C.-H.; Moizan-Baslé, V.; Nieto, C.; Amrouche, H.; Bats, N.; Audebrand, N.; Farrusseng, D. Facile synthesis of an ultramicroporous MOF tubular membrane with selectivity towards CO2. *New J. Chem.* **2011**, *35* (1), 41−44.
(11) Brown, A. J.; Johnson, J.; Lydon, M. E.; Koros, W. J.; Jones, C. W.; Nair, S. Continuous polycrystalline zeolitic imidazolate framework-90 membranes on polymeric hollow fibers. *Angew. Chem., Int. Ed.* **2012**, *51* (42), 10615−10618.
(12) Ge, L.; Zhou, W.; Du, A.; Zhu, Z. Porous polyethersulfone-supported zeolitic imidazolate framework membranes for hydrogen separation. *J. Phys. Chem. C* **2012**, *116* (24), 13264−13270.
(13) Li, J.-R.; Sculley, J.; Zhou, H.-C. Metal-organic frameworks for separations. *Chem. Rev.* **2011**, *112* (2), 869−932.
(14) Pan, Y.; Wang, B.; Lai, Z. Synthesis of ceramic hollow fiber supported zeolitic imidazolate framework-8 (ZIF-8) membranes with high hydrogen permeability. *J. Membr. Sci.* **2012**, *421−422*, 292−298.
(15) Xu, G.; Yao, J.; Wang, K.; He, L.; Webley, P. A.; Chen, C.-S.; Wang, H. Preparation of ZIF-8 membranes supported on ceramic hollow fibers from a concentrated synthesis gel. *J. Membr. Sci.* **2011**, *385*, 187−193.
(16) Yang, T.; Shi, G. M.; Chung, T. S. Symmetric and asymmetric zeolitic imidazolate frameworks (ZIFs)/polybenzimidazole (PBI) nanocomposite membranes for hydrogen purification at high temperatures. *Adv. Energy Mater.* **2012**, *2* (11), 1358−1367.
(17) Yao, J.; Li, L.; Wong, W. H. B.; Tan, C.; Dong, D.; Wang, H. Formation of ZIF-8 membranes and crystals in a diluted aqueous solution. *Mater. Chem. Phys.* **2013**, *139* (2−3), 1003−1008.
(18) Zhou, S.; Zou, X.; Sun, F.; Zhang, F.; Fan, S.; Zhao, H.; Schiestel, T.; Zhu, G. Challenging fabrication of hollow ceramic fiber supported $Cu_3(BTC)_2$ membrane for hydrogen separation. *J. Mater. Chem.* **2012**, *22* (20), 10322−10328.
(19) Hu, Y.; Dong, X.; Nan, J.; Jin, W.; Ren, X.; Xu, N.; Lee, Y. M. Metal-organic framework membranes fabricated via reactive seeding. *Chem. Commun.* **2011**, *47* (2), 737−739.
(20) Venna, S. R.; Carreon, M. A. Microwave assisted phase transformation of silicoaluminophosphate zeolite crystals. *J. Mater. Chem.* **2009**, *19* (20), 3138−3140.
(21) Mao, Y.; Shi, L.; Huang, H.; Cao, W.; Li, J.; Sun, L.; Jin, X.; Peng, X. Room temperature synthesis of free-standing HKUST-1 membranes from copper hydroxide nanostrands for gas separation. *Chem. Commun.* **2013**, *49*, 5666−5668.
(22) Wang, D.; Li, K.; Teo, W. Preparation and characterization of polyvinylidene fluoride (PVDF) hollow fiber membranes. *J. Membr. Sci.* **1999**, *163* (2), 211−220.
(23) Yu, Q.; Huang, H.; Chen, R.; Wang, P.; Yang, H.; Gao, M.; Peng, X.; Ye, Z. Synthesis of CuO nanowalnuts and nanoribbons from aqueous solution and their catalytic and electrochemical properties. *Nanoscale* **2012**, *4* (8), 2613−2620.
(24) Luo, Y.-H.; Huang, J.; Jin, J.; Peng, X.; Schmitt, W.; Ichinose, I. Formation of positively charged copper hydroxide nanostrands and their structural characterization. *Chem. Mater.* **2006**, *18* (7), 1795−1802.
(25) Yoo, Y.; Lai, Z.; Jeong, H.-K. Fabrication of MOF-5 membranes using microwave-induced rapid seeding and solvothermal secondary growth. *Microporous Mesoporous Mater.* **2009**, *123* (1), 100−106.
(26) Shah, M.; McCarthy, M. C.; Sachdeva, S.; Lee, A. K.; Jeong, H.-K. Current status of metal-organic framework membranes for gas separations: Promises and challenges. *Ind. Eng. Chem. Res.* **2012**, *51* (5), 2179−2199.
(27) Guo, H.; Zhu, G.; Hewitt, I. J.; Qiu, S. "Twin Copper Source" growth of metal-organic framework membrane: $Cu_3(BTC)_2$ with high permeability and selectivity for recycling H_2. *J. Am. Chem. Soc.* **2009**, *131* (5), 1646−1647.
(28) Guerrero, V. V.; Yoo, Y.; McCarthy, M. C.; Jeong, H.-K. HKUST-1 membranes on porous supports using secondary growth. *J. Mater. Chem.* **2010**, *20* (19), 3938−3943.
(29) Huang, A.; Caro, J. Covalent post-functionalization of zeolitic imidazolate framework ZIF-90 membrane for enhanced hydrogen selectivity. *Angew. Chem., Int. Ed.* **2011**, *50* (21), 4979−4982.
(30) Huang, A.; Dou, W.; Caro, J. Steam-stable zeolitic imidazolate framework ZIF-90 membrane with hydrogen selectivity through covalent functionalization. *J. Am. Chem. Soc.* **2010**, *132* (44), 15562−15564.
(31) Mao, Y.; Cao, W.; Li, J.; Sun, L.; Peng, X. HKUST-1 membranes anchored on porous substrate by hetero MIL-110 nanorod array seeds. *Chem.—Eur. J.* **2013**, *19* (36), 11883−11886.
(32) Nan, J.; Dong, X.; Wang, W.; Jin, W.; Xu, N. Step-by-step seeding procedure for preparing HKUST-1 membrane on porous α-alumina support. *Langmuir* **2011**, *27* (8), 4309−4312.
(33) Pan, Y.; Lai, Z. Sharp separation of C2/C3 hydrocarbon mixtures by zeolitic imidazolate framework-8 (ZIF-8) membranes synthesized in aqueous solutions. *Chem. Commun.* **2011**, *47* (37), 10275−10277.
(34) Huang, A.; Chen, Y.; Wang, N.; Hu, Z.; Jiang, J.; Caro, J. A highly permeable and selective zeolitic imidazolate framework ZIF-95 membrane for H_2/CO_2 separation. *Chem. Commun.* **2012**, *48* (89), 10981−10983.